Pair breaking versus symmetry breaking: Origin of the Raman modes in superconducting cuprates

N. Munnikes,[1,*] B. Muschler,[1] F. Venturini,[1,†] L. Tassini,[1,‡] W. Prestel,[1,§] Shimpei Ono,[2] Yoichi Ando,[3] D. C. Peets,[4,*] W. N. Hardy,[4,5] Ruixing Liang,[4,5] D. A. Bonn,[4,5] A. Damascelli,[4,5,‖] H. Eisaki,[6,‖] M. Greven,[7,‖] A. Erb,[1] and R. Hackl[1]

[1]*Walther Meissner Institute, Bavarian Academy of Sciences and Humanities, 85748 Garching, Germany*

[2]*Central Research Institute of the Electric Power Industry, Komae, Tokyo 201-8511, Japan*

[3]*Institute of Scientific and Industrial Research, Osaka University, Ibaraki, Osaka 567-0047, Japan*

[4]*Department of Physics and Astronomy and Quantum Matter Institute, University of British Columbia, Vancouver, Canada, BC V6T 1Z4*

[5]*Canadian Institute for Advanced Research, Toronto, Canada, M5G 1Z8*

[6]*Nanoelectronic Research Institute, AIST, Tsukuba 305-8568, Japan*

[7]*School of Physics and Astronomy, University of Minnesota, Minneapolis, Minnesota 55455, USA*

(Received 9 June 2011; revised manuscript received 22 August 2011; published 28 October 2011)

We performed Raman scattering experiments on superconductivity-induced features in $Bi_2Sr_2(Ca_{1-x}Y_x)Cu_2O_{8+\delta}$ (Bi-2212), $YBa_2Cu_3O_{6+x}$ (Y-123), and $Tl_2Ba_2CuO_{6+\delta}$ (Tl-2201) single crystals. The results in combination with earlier ones enable us to systematically analyze the spectral features in the doping range $0.07 \leqslant p \leqslant 0.24$. In B_{2g} (xy) symmetry, we find universal spectra and the maximal gap energy Δ_0 to scale with the superconducting transition temperature T_c. The B_{1g} (x^2-y^2) spectra in all three compounds show an anomalous increase of the intensity toward overdoping. The energy scale of the corresponding peak is neither related to the pairing energy nor to the pseudogap, but possibly stems from a symmetry breaking transition at the onset point of superconductivity at $p_{sc2} \simeq 0.27$.

DOI: 10.1103/PhysRevB.84.144523 PACS number(s): 74.72.−h, 74.20.Mn, 74.25.Gz, 78.30.−j

I. INTRODUCTION

The magnitude of the gap in the quasiparticle excitation spectrum determines the energy difference between the superconducting and the normal state. The momentum dependence $\Delta_{\mathbf{k}} = \Delta_0 f(\mathbf{k})$ reflects properties of the pairing potential. In the case of the copper-oxygen (cuprate) superconductors the d-wave character of the gap is well established,[1] suggesting the influence of repulsive contributions to the pairing interaction,[2–4] while the energy scales, in particular, as a function of (hole) doping p with $p = 1 - n$ the number of mobile holes per planar Cu atom, remain elusive. There are substantial differences between the overall behavior in the areas close to $(\pi,0)$ and equivalent points (antinode) and $(\pi/2,\pi/2)$ (node) in the Brillouin zone (BZ) of the CuO_2 planes, which are hard to pin down experimentally. The theoretical interpretation is accordingly controversial. While the nodal gap is believed to reflect more or less the pairing interaction, the antinodal energy scale probably originates from a rather complex interrelation of superconductivity and another instability.[5–7] This holds particularly true for the underdoped range, $p \leqslant 0.16$. In some experiments the maximum of the superconducting gap $\Delta_0(p)$ is found to stay essentially constant in wider doping ranges around $p = 0.16$ and to decrease only close to the end points p_{sc1} and p_{sc2} of the superconducting dome.[8,9] Other experiments indicate $\Delta_0(p)$ to more or less follow the superconducting transition temperature T_c.[10–16] Finally, studies of the heat transport indicate that $\Delta_0(p)$ decreases continuously with increasing doping.[17–21]

Below $T^* > T_c$, a second energy gap $\Delta^*(p)$ opens up. Δ^* is the typical range over which spectral weight is suppressed in the vicinity of the antinodal points of the BZ and is usually referred to as the pseudogap.[5,22–25] In the spectroscopic experiments, T_c and the pseudogap temperature T^* are found to become indistinguishable in the experiment-dependent range $0.15 < p^* < 0.20$. However, there still remain two energy scales below T_c exhibiting different doping dependences.[5,10,12,13,25–27] The scale observed close to the BZ diagonal appears to follow T_c quite closely in those experiments, which, as pointed out first by Deutscher,[13] probe the condensate such as Andreev reflection or electronic Raman scattering. The antinodal scale is approximately proportional to $(1 - p/p_0)$ with $0.20 < p_0 < 0.30$ and was first identified in the quasiparticle spectrum[13,28,29] but also anticipated from Raman experiments on the overdoped side.[30] The functional dependence on p, yet not necessarily the magnitude, of this scale is remarkably similar to that of $\Delta^*(p)$ (for more details see Refs. 7 and 25). However, above p^* there is no longer any suppression of spectral weight in the normal state,[8–10,12,14–16,25,27,30–32] and superconducting coherence peaks are observed everywhere on the Fermi surface by angle-resolved photoemission (ARPES)[9,26,32] and, independent of the location on the sample surface, by scanning tunneling spectroscopy (STS).[8,27,33]

The wide ranges of the characteristic doping levels p^* and p_0 as well as of the energy scales $\Delta^*(p)$ and $\Delta_{\mathbf{k}}(p)$ are not fully explored yet. There are indications of a dependence on the material class, the samples, and also on the experimental probe. The pseudogap $\Delta^*(p)$ was first observed by optical (IR) conductivity in $YBa_2Cu_3O_{6+x}$ (Y-123) with light polarized along the c axis.[22] Given the band structure of Y-123 this experiment emphasizes the antinode.[34,35] Soon thereafter, an antinodal gap above T_c was observed in ARPES experiments.[23,24] In Raman experiments, two types of gaplike features are found in the B_{1g} and B_{2g} symmetries[10,14,36,37] for $p < 0.21$. An intensity suppression in B_{2g} symmetry of order 5–10% occurs below T^* in an almost doping independent energy range of approximately 100 meV (800 cm^{-1})[10,14,36] comparable to the exchange energy J. In B_{1g} symmetry, the Raman intensity is suppressed in an energy range up to at least 200 meV with the suppression setting in abruptly below

$p \approx 0.21$.[37,38] In the same doping range, the superfluid density starts to decrease,[6] and an asymmetry with respect to zero bias of the scanning tunneling spectra develops for specific locations on the crystals.[8,27,33,39] Also below T_c, the spectra develop a strong dependence on location. In some areas, there are still coherence peaks while in other spots a much larger gap without well-defined peaks is observed. The distribution of gaps becomes wider and ranges from 5 to 12 in units of $k_B T_c$.

In a recent Raman experiment, the energy of the antinodal pair-breaking peak of fully oxygenated $YBa_2Cu_3O_{\sim 7}$ was studied as a function of applied pressure.[40] The superconductivity-induced peak position decreases by approximately 50% in the pressure range up to 22.3 GPa, while T_c changes only by 25%.[40,41] In units of $k_B T_c$, the position of the peak moves from 6.2 at ambient pressure to 4.2 at 22.3 GPa. Particularly the last result casts doubt on the prevailing interpretation of the B_{1g} Raman spectra in the superconducting state in terms of a direct relationship to the pairing energy or the pseudogap.

In this paper, we present new electronic Raman scattering experiments on Y-123, $Bi_2Sr_2(Ca_{1-x}Y_x)Cu_2O_{8+\delta}$ (Bi-2212), and $Tl_2Ba_2CuO_{6+\delta}$ (Tl-2201) and put them into context with earlier results. We systematically study the sample dependence and, as an additional variable, the intensity of the superconductivity-induced features for doping levels $0.07 \leqslant p \leqslant 0.24$. The results in B_{2g} symmetry show that the momentum dependence of the superconducting gap, $f(\mathbf{k}) = \Delta_{\mathbf{k}}/\Delta_0$, hardly depends on doping for either Y-123 or Bi-2212. For $p > 0.16$, the antinodal spectra of Bi-2212 reflect neither the pseudogap nor the superconducting gap. Rather, the doping dependence of both the intensity and the energy of the superconductivity-induced modes suggests that it is closely related to the onset point of superconductivity at $p_{sc2} = 0.27$ on the very overdoped side of the phase diagram.

The paper is organized as follows: in Sec. II, we describe details of the experiment, the samples studied here as well as those investigated in our earlier work. In Sec. III, we describe in detail the results of the new experiments with the emphasis placed on the comparison of samples with nearly equal transition temperatures. In Sec. IV, we compile and discuss the results of most of our experiments obtained over the years. The energy scales are compared to the results from other Raman groups and to those from ARPES and STS. In Sec. V, we summarize our results and conclusions and formulate open questions.

II. EXPERIMENT AND SAMPLES

Momentum-dependent electron dynamics such as electron-hole excitations in normal metals, gaps in superconductors, or collective modes can be studied by Raman scattering via the intracell fluctuations of the charge density excited by the photons. As a consequence, different parts of the Brillouin zone (BZ) can be projected out independently by appropriately adjusting the polarizations of the incoming and outgoing photons.[42] In the cuprates, B_{1g} and B_{2g} spectra emphasize antinodal and nodal electrons, respectively, with the form factors shown in the insets of Figs. 1(a) and 1(b). Collective excitations with pure symmetries can be accessed separately. In the superconducting state, the condensate is directly probed, since the anomalous part of the Green function is measured in addition to the normal one.[42–45]

The spectra were measured with standard Raman equipment using the Ar^+ line at 458 nm and, for $Tl_2Ba_2CuO_{6+\delta}$, at 514 nm. The temperatures generally refer to the illuminated spot and are typically between 5 and 10 K above those of the sample holder as determined from the comparison of energy-gain and loss spectra. All spectra shown here are Raman response functions $R\chi''_{I,S}(\Omega,T)$, where I and S refer to incoming and scattered photons. $R\chi''_{I,S}(\Omega,T)$ is obtained from the cross section via the fluctuation-dissipation theorem to remove trivial temperature dependences. This means that the experimental intensity is divided by the thermal Bose factor, $\{1 + n(\Omega,T)\} = [e^{-\hbar\Omega/k_B T} - 1]^{-1}$, after having been corrected for the sensitivity of the instrument and multiplied by ω_I/ω_S. $\Omega = \omega_I - \omega_S$ is the energy transferred from the photons to the system. The polarizations of the incoming and scattered photons $\mathbf{e}_I$ and $\mathbf{e}_S$ are always indicated symbolically by two arrows and referred to as xy and $x'y'$ using Porto notation with $x' = 1/\sqrt{2}(1,1)$ and $y' = 1/\sqrt{2}(1,-1)$. The constant R absorbs experimental factors and converts the units of $\chi'' = \Im\chi$ into (counts s^{-1} mW^{-1}). All spectra displaying $R\chi''_{I,S}(\Omega,T)$ can be compared on an absolute scale.

The samples studied here were prepared in Garching, Stanford, Tokyo, and Vancouver (see Table I). $(Y_{0.92}Ca_{0.08})Ba_2Cu_3O_{6.3}$ (Y-UD28) single crystals were grown in $BaZrO_3$ crucibles using starting materials with purities of better than 99.999% (5N). In this way, ultrahigh quality samples can be obtained.[50,51] The $Bi_2Sr_2CaCu_2O_{8+\delta}$ (Bi-OPT94) and $Bi_2Sr_2(Ca_{0.92}Y_{0.08})Cu_2O_{8+\delta}$ (Bi-OPT96) single crystals were prepared by the floating zone method in the mirror furnace.[46] $Tl_2Ba_2CuO_{6+\delta}$ (Tl-OD78 and Tl-OD46) were prepared in alumina crucibles.[47] The parameters of the freshly prepared samples are compiled in Table I (a–g). Since one of the central messages of the paper is the dependence of the B_{1g} results on details of the samples, it is crucial to compare the new results to those obtained earlier on different sample sets [Table I (h–t)] under comparable conditions.

III. RESULTS

We plot raw data of new measurements on high-quality single crystals of $(Y_{0.92}Ca_{0.08})Ba_2Cu_3O_{6.3}$ (Y-UD28, $T_c = 28$ K) in Figs. 1(a) and 1(b), $Bi_2Sr_2CaCu_2O_{8+\delta}$ (Bi-OPT94, $T_c = 94$ K) in Figs. 1(e) and 1(f), and $Bi_2Sr_2(Ca_{0.92}Y_{0.08})Cu_2O_{8+\delta}$ (Bi-OPT96, $T_c = 96$ K; Bi-OD87, $T_c = 87$ K) in Figs. 1(c), 1(d), 1(g), and 1(h). Shown are spectra right above and well below the transition temperature T_c. In spite of the almost identical T_cs, the two optimally doped Bi-2212 samples [see Figs. 1(c)–1(f)] exhibit substantial differences in the B_{1g} spectra (c,e) at $T \to 0$. The peak energy $\Omega^{B1g}_{\text{peak}}$ of sample Bi-OPT96 is approximately 25% higher than that of Bi-OPT94, while T_c differs only by 2%. The variation of the peak position is accompanied by a change in the amplitude A_{sc}, i.e., the difference between the superconducting and the normal-state spectra at the peak maximum, by a factor of 2.7. On the other hand, the B_{2g} spectra exhibit only minor changes in shape, amplitude, and peak energy.

TABLE I. Complete list of samples used for Raman scattering. In rows (a–g), we describe samples measured in this study. In rows (h–t), the properties of samples studied earlier are compiled. Samples (a, b, h, i, and j) were prepared by A. Erb (WMI Garching), (c and s) by Shimpei Ono and Yoichi Ando (CRIEPI, Tokyo and Osaka University), (d and e) by A. Damascelli, H. Eisaki, and M. Greven (Stanford, Ref. 46, and Vancouver), (f and g) by D. C. Peets, W. N. Hardy, R. Liang, and D. A. Bonn (Vancouver, Ref. 47), (k, l, and t) by H. Berger and L. Forró (EPFL, Lausanne, Refs. 10 and 37), (m–r) by B. Revaz (University Geneva, Refs. 14 and 37). The transition temperatures were measured resistively (k, l, and t) via magnetometry (h–j, d, and m–o) or via the nonlinear ac response (a–g and p–s). Hence, in some cases we used two methods and found good agreement of T_c values when appropriately defined. In the cases of resistivity and linear susceptibility measurements, the transition widths are defined by the 10 and 90% points. If only the nonlinear susceptibility was measured, ΔT_c is estimated from the shape of the signal close to T_c, and the uncertainty can be as large as 50%. All doping levels p are derived from T_c via the relation $p = 0.16 \mp 0.11\sqrt{1 - T_c/T_c^{\max}}$ using $T_c^{\max} = 94$ K.[48] The resulting error is of order ± 0.01. In Y-123 (and, probably, also in Bi-2212), the experimental T_c is systematically below the parabola in the vicinity of the 1/8 anomaly[49] making the determination of $p(T_c)$ less precise between 0.10 and 0.15.

label	sample	sample ID	doping	T_c (K)	ΔT_c (K)
a	$(Y_{0.92}Ca_{0.08})Ba_2Cu_3O_{6.3}$	Y-UD28	0.07	28	2
b	$YBa_2Cu_3O_{6.4}$	Y-UD29	0.07	28	3
c	$Bi_2Sr_2CaCu_2O_{8+\delta}$	Bi-OPT94	0.16	94	2
d	$Bi_2Sr_2(Ca_{0.92}Y_{0.08})Cu_2O_{8+\delta 1}$	Bi-OPT96	0.16	96	2
e	$Bi_2Sr_2(Ca_{0.92}Y_{0.08})Cu_2O_{8+\delta 2}$	Bi-OD87	0.19	87	2
f	$Tl_2Ba_2CuO_{6+\delta}$	Tl-OD78	0.21	78	5
g	$Tl_2Ba_2CuO_{6+\delta}$	Tl-OD46	0.24	46	5
h	$YBa_2Cu_3O_{6.5}$	Y-UD60	0.10	58	5
i	$YBa_2Cu_3O_{6.93}$	Y-OPT93	0.16	93	0.5
j	$YBa_2Cu_3O_{6.99}$	Y-OD87	0.18	87	2
k	$Bi_2Sr_2(Ca_{0.62}Y_{0.38})Cu_2O_{8+\delta}$	Bi-UD58	0.10	58	5
l	$Bi_2Sr_2CaCu_2O_{8+\delta}$	Bi-UD92	0.15	91.7	–
m	$Bi_2Sr_2CaCu_2O_{8+\delta}$	Bi-OPT92	0.16	92	1
n	$Bi_2Sr_2CaCu_2O_{8+\delta}$	Bi-OD82	0.20	82	3
o	$Bi_2Sr_2CaCu_2O_{8+\delta}$	Bi-OD78	0.21	77.8	0.2
p	$Bi_2Sr_2CaCu_2O_{8+\delta}$	Bi-OD65	0.22	65	1
q	$Bi_2Sr_2CaCu_2O_{8+\delta}$	Bi-OD62	0.22	62	1
r	$Bi_2Sr_2CaCu_2O_{8+\delta}$	Bi-OD56	0.23	56	5
s	$Bi_2Sr_2CaCu_2O_{8+\delta}$	Bi-OD56	0.23	56	5
t	$Bi_2Sr_2CaCu_2O_{8+\delta}$	Bi-OD55	0.23	55	5

The overdoped sample Bi-OD87 [see Figs. 1(g) and 1(h)] was prepared from Bi-OPT96 by oxygen annealing. Both peak frequencies move downward along with T_c, with a tendency of the B_{1g} peak to move more rapidly than the B_{2g} peak as observed earlier in Bi-2212,[14,15,30,37] Y-123,[10,14,52,53] and $HgBa_2CuO_{6+\delta}$.[16]

On the underdoped side, we studied Y-123 for its superior crystal quality.[50] We find superconductivity to be observable only in B_{2g} symmetry. The peak energy is at approximately one third of that observed at optimal doping and follows T_c. The absence of superconductivity-induced peaks in B_{1g} symmetry appears to be a generic feature of underdoped cuprates with $p \leqslant 0.13$ (for a discussion see Ref. 42), which occurs approximately in the same doping range as the loss of coherence close to the antinodal points[26,54] and the loss of spectral weight in the oxygen K edge absorption.[55,56]

In Fig. 2, we show results on a freshly prepared set[47] of high-quality $Tl_2Ba_2CuO_{6+\delta}$ single crystals at $p = 0.21$ and $p = 0.24$ on the overdoped side, Tl-OD78 and Tl-OD46, with transition temperatures of 78 and 46 K, respectively. The crystals were relatively small with maximal dimensions of less than 1 mm. The spectra were measured on as-grown surfaces since cleaving was not attempted for the small number of samples available. Residual flux and adsorbates lead to a contribution from the laser line (at $\Omega = 0$) extending to energies as high as 50–100 cm^{-1} [see in particular Fig. 2(d)] and temperature-dependent variations of the overall Raman intensity in the range $\pm 20\%$. Consequently, the overall intensities are not as quantitative as those of Y-123 and Bi-2212 with a stability of better than $\sigma = 5$ %. By using the laser line at 514 nm, the cross sections of Tl-2201 become comparable to those of Y-123 and Bi-2212 and do not depend significantly on doping. With excitation at 458 nm resonance effects enhance the absolute intensity in Tl-OD78 by almost a factor of two over that measured with the line at 514 nm. Similar changes for both the continuum and the superconductivity-induced peaks have been reported earlier for excitation between 416 and 755 nm.[57] Kang *et al.* showed also that the resonances essentially disappear for wavelengths $\lambda \geqslant 514$ nm. Therefore it is safe to conclude that the relative change of the normalized B_{1g} pair-breaking intensity is close to two for the doping levels studied here.

The B_{1g} peaks are clearly resolved and found at 370 and 120 cm^{-1} for Tl-OD78 and Tl-OD46 corresponding to 6.8 and 3.7 $k_B T_c$, respectively. The B_{2g} peaks are very weak, with maxima close to those in B_{1g}. While the energy for Tl-OD78 is in the same range as in Bi-2212, that of Tl-OD46 is smaller than in any other sample studied here. However, low peak energies at doping levels above 0.22 have been observed before.[11,57,58] Only Gasparov *et al.* measured both the B_{1g} and

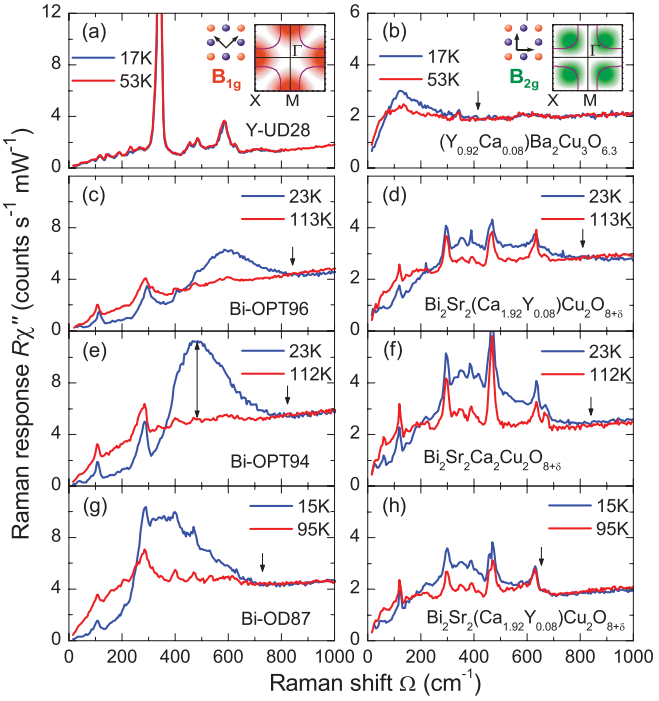

FIG. 1. (Color online) Raman response $R\chi''(\Omega,T)$ (raw data): (a) and (b) $(Y_{0.92}Ca_{0.08})Ba_2Cu_3O_{6.3}$ (Y-UD28) and (c)–(h) $Bi_2Sr_2(Ca_{1-x}Y_x)Cu_2O_{8+\delta}$ (Bi-OPT94, Bi-OPT96, and Bi-OD87), in B_{1g} and B_{2g} symmetries as indicated. The corresponding light polarizations and sensitivities in the Brillouin zone are shown in the insets with copper and oxygen atoms displayed in red and blue, respectively. In (e), a double-headed arrow indicates the amplitude A_{sc} of the superconductivity-induced peak. Whenever applicable, a down-pointing arrow gives the approximate position where normal-state and superconducting spectra merge.

the B_{2g} channel, and they observed peak energies and relative intensities close to those here. For Tl-OD46, the analysis of the B_{2g} peak yields a lineshape similar to that of the B_{1g} mode. This suggests a polarization leakage originating from either a misorientation by approximately 4° or from internal strain fields and an orthorhombic distortion in Tl-2201.[59–61] We note that the orthorhombic distortion is not larger than 1% and is not enough to explain the leakage. It is concluded that a quantitative analysis of the B_{2g} spectra of Tl-2201 is premature. The change in energy and intensity of the B_{1g} mode as a function of doping seems to be robust and in qualitative agreement with the published literature. The variation of the intensity will be of particular interest later.

IV. DISCUSSION

A. Energy scales derived from the B_{2g} spectra

Figure 1 shows that the B_{2g} peak energies in the superconducting state follow T_c as pointed out earlier in various publications.[10,13–15,37,42,52,62,63] Beyond that, we demonstrate here that the entire B_{2g} spectra can be scaled by normalizing the energy axis of each sample to the respective experimentally determined T_c (N.B., not the doping p, which is a derived quantity) and the intensity to unity at energies in the range 800–1000 cm^{-1}. As shown in Fig. 3, the superconducting

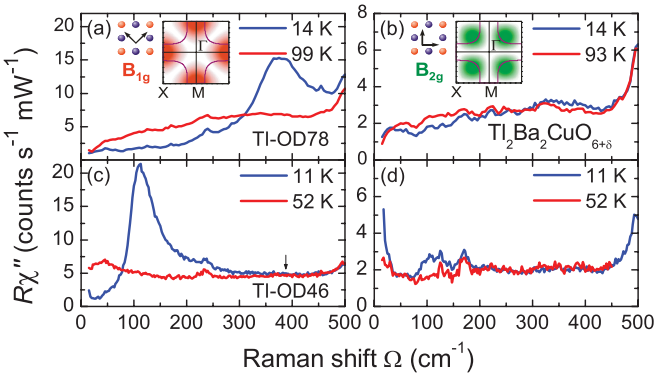

FIG. 2. (Color online) Raman response $R\chi''(\Omega,T)$ of $Tl_2Ba_2CuO_{6+\delta}$ with $T_c = 78$ K (Tl-OD78) [panels (a) and (b)] and $T_c = 46$ K (Tl-OD46) [panels (c) and (d)]. Note that the energy scales are different from those in Fig. 1. The spectra were measured with the laser line at 514 nm. The superconducting spectra were multiplied by constant scaling factors s_0 in the range $0.9 \leqslant s_0 \leqslant 1.1$ to match the intensities above the pair-breaking range with those in the normal state.

B_{2g} spectra collapse on universal curves for both Y-123 and Bi-2212. We note that the B_{2g} spectrum of Tl-OD46 is not consistent with this picture [see Fig. 2], while $HgBa_2CuO_{4+\delta}$ (Hg-1201) at $p = 0.24$ fits reasonably well.[63] The reasons for the discrepancies of Tl-OD46 are given in Sec. III and are not considered sufficiently significant to challenge the scaling argument. Further work is needed here.

The low-energy part of the normalized spectra can be described quantitatively in terms of a $d_{x^2-y^2}$ gap.[64] Naturally, the description fails at higher energies, since only the weak coupling limit is considered, which neglects the strong interactions responsible for the large self-energy of the electrons[26] and, hence, the Raman spectra at high energies.[42,65] With the gap represented by

$$\Delta_{\mathbf{k}} = \frac{\Delta_0}{2}(\cos k_x - \cos k_y), \tag{1}$$

we find agreement between theory and experiment up to and slightly beyond the pair-breaking peak (see Fig. 3). As shown recently for optimal doping, the range of agreement between the Raman spectra and the d-wave prediction can be extended if the self-energy effects such as observed by ARPES[26,66] are included using a strong-coupling approach.[65]

While the B_{2g} maximum $\Omega_{\text{peak}}^{B2g}(p)$ itself scales approximately as $6\,k_BT_c$ consistent with previous reports (see references above), the gap maximum Δ_0 from the d-wave fit in Fig. 3 follows T_c as

$$2\Delta_0(p) = (9.3 \pm 0.5)\,k_BT_c(p) \tag{2}$$

corresponding to approximately twice the canonical weak-coupling BCS result of 4.21 for a two-dimensional d-wave gap. Thus the B_{2g} spectra of high-quality Y-123 and Bi-2212 samples provide a wealth of evidence that both the gap ratio Δ_0/k_BT_c as seen by Raman scattering and the momentum dependence $f(\mathbf{k})$ remain unchanged throughout the entire doping range studied ($0.07 \leqslant p \leqslant 0.23$). Similar conclusions may apply to Hg-1201[63] although the scaling was not attempted.

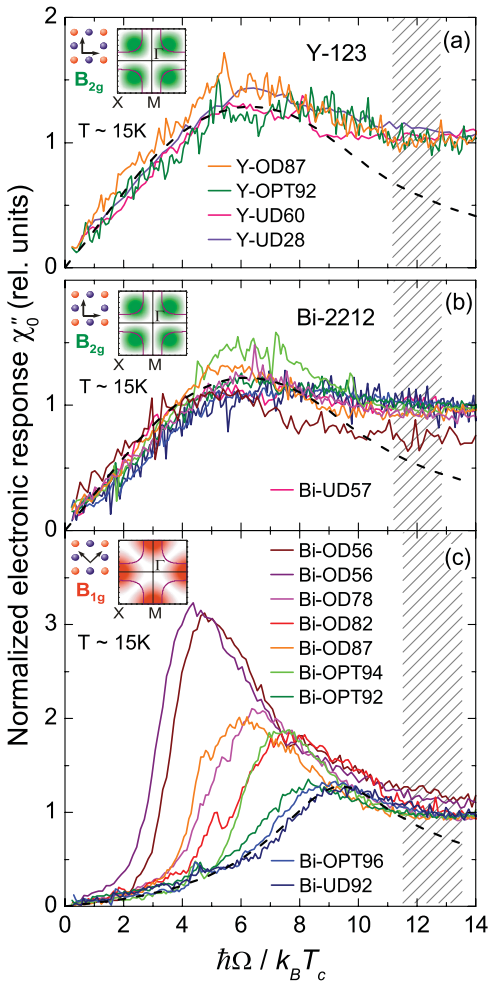

FIG. 3. (Color) Normalized electronic Raman response $\chi_0''(\Omega, p)$ (phonons subtracted) of $(Y_{1-y}Ca_y)Ba_2Cu_3O_{6+x}$ in B_{2g} symmetry (a), $Bi_2Sr_2(Ca_{1-x}Y_x)Cu_2O_{8+\delta}$ in B_{2g} (b), and B_{1g} symmetry (c). Spectra from samples other than those shown in Fig. 1 are taken from our published work.[10,14,37,53] For clarity, the phonons have been subtracted. The energy axes are normalized to the individual transition temperatures. All superconducting spectra merge with the normal-state response in the shaded range. The theoretical weak-coupling pair-breaking spectra (dashed lines) are the Tsuneto function on a realistic band structure weighted with the vertices for B_{1g} and B_{2g} symmetry. $2\Delta_0 = 9.3\, k_B T_c$ and a phenomenological broadening of 20% was used.

The weak dependence of the B_{2g} spectra on sample details can be explained straightforwardly by small changes in the concentration of scattering centers[67] resulting from defects or quenched disorder, for instance.[46] The doping independence of the normalized B_{2g} spectra includes the intensity, the position, and the shape of the superconducting peaks (see Figs. 1 and 3).

B. Interrelation of B_{1g} and B_{2g} spectra

The doping dependence of the B_{2g} spectra imposes constraints on the interpretation of the B_{1g} spectra since the two symmetries are linked by the form factors.[42] A potential change in the momentum dependence $f(\mathbf{k})$ of the gap would inevitably leave imprints on both the B_{1g} and B_{2g} spectra demonstrating that the disappearance of the B_{1g} gap structures for $p < 0.15$ [see, e.g., Fig. 1(a)] is an effect, which, to the resolution possible in this experiment, is occurring in the B_{1g} symmetry alone. This conclusion is supported by the results in the normal state. For $p > 0.21 \pm 0.01$, the spectra and, in particular, the electronic relaxation rates are essentially isotropic.[54,62] For $p \leqslant 0.21$, the anisotropy between the symmetries develops almost abruptly.[54] With less resolution in p, this was corroborated recently for Hg-1201,[16] Bi-2212,[38] $La_{2-x}Sr_xCuO_4$ (LSCO), and Tl-2201.[68]

Below $p \simeq 0.21$, the oxygen K edge absorption, which, supposedly, is related to the number of holes, starts to decrease[55,56] suggesting a transition between metal and Mott physics. Similarly, $p = 0.21$ is close to $p = 0.23$ where recent ARPES experiments on Y-123 indicate that not only the antinodal but also the nodal quasiparticle weight Z_N starts to decrease.[69] In earlier ARPES studies below T_c, the spectral weight was observed to be lost predominantly at the antinode for $p \leqslant 0.18$ (Refs. 32 and 70). More recently, ARPES studies on Tl-2201 indicated a further sharpening of the antinodal quasiparticle peak for doping levels above $p = 0.21$ which, however, is more likely to originate from a reduced quasiparticle scattering rate Γ_{AN} than from a further increase of the weight Z_{AN} (see Ref. 71). For $p < 0.15$, the Fermi surface shrinks to arcs in the vicinity of the nodal direction[69,72] although, at least for LSCO, neither is the spectral weight at the antinode completely lost for $p > 0.03$ nor are there rapid changes in the weight at specific k points.[73,74] A loss of coherent quasiparticle weight is also observed in the specific heat[6] and in the tunneling spectra.[8,27,33]

The reduction of Z_{AN} is in at least qualitative agreement with the variation of the B_{1g} spectra in the normal state, which, for p decreasing from 0.21 to 0.16, loose 30 to 40% of their spectral weight in the range up to 2000 cm^{-1} and change their shape.[54,63] In contrast, in B_{2g} symmetry, the shape is by and large conserved and the overall intensity even increases by approximately 20% (Refs. 14 and 75). This observation is at variance with the reduction of the nodal quasiparticle weight Z_N[69] at least when the Raman continuum is considered to originate from particle-hole excitations in the lowest order approximation. We emphasize that the spectral changes in B_{1g} symmetry have to be distinguished clearly from the influence of the pseudogap on the B_{2g} spectra for $T < T^*$ which is a 5–10% effect in the range up to 800 cm^{-1} (Refs. 10,14,36, and 76). Already the different energy ranges indicate that the gaplike phenomena in B_{1g} and B_{2g} symmetry cannot have the same origin. Apparently, the dichotomy between the energy ranges and spectral weight changes is the generic behavior if (i) the samples are sufficiently clean and (ii) resonance effects are unimportant (see above and Ref. 68). Hence, from the viewpoint of a very large set of Raman data, the substantial loss of spectral weight both above and below T_c is a peculiarity of the B_{1g} symmetry.

Our interpretation of this dichotomy between B_{1g} and B_{2g} symmetry in terms of two independent phenomena is not generally shared. Chen,[52] Le Tacon,[16] and Blanc[63] and coworkers interpret the suppression of the B_{1g} and the small changes of the B_{2g} pair-breaking features in terms of a gradual loss of quasiparticle weight starting at the antinode as qualitatively observed by ARPES. In this scenario, 100% of the B_{1g} and

50 to 80% of the B_{2g} intensities are predicted to be lost[63] toward underdoping. However, this interpretation cannot easily be reconciled with the experimental observations found consistently in four cuprate families[68] since, as mentioned above, the B_{2g} spectra in the normal state (including $T < T^*$) are largely doping independent. We believe that one has to go beyond the lowest-order particle-particle correlation function for the Raman response to resolve the apparent discrepancies between single- and two-particle properties.

To summarize this part, the Raman spectra in B_{1g} and B_{2g} symmetry both in the normal and the superconducting state exhibit distinctly different doping dependences occurring in rather different energy ranges, which make it difficult to explain that they have the same origin. We rather argue that the suppression of spectral weight in B_{1g} symmetry is linked to the correlation or Mott gap[54,77] while the effects of the pseudogap are observed predominantly in B_{2g} symmetry and are relatively small.[10,14,36,76] In the narrow doping range $0.12 < p < 0.16$, there may also be effects of the pseudogap on the B_{1g} spectra[38] before any relationship to the carriers is quenched by the correlation gap below $p \sim 0.12$. On the other hand, symmetry protects the Fermi-liquid-like state of the nodal electrons down to $p \simeq 0.05$ where superconductivity disappears. For $p \lesssim 0.05$, the overall B_{2g} intensity decreases essentially linearly with doping before it vanishes at $p = 0$.[75] Presently, we cannot provide a microscopic model for the selective suppression of the B_{1g} spectra neither in the superconducting nor in the normal state.[54] Yet, the inclusion of higher order diagrams with symmetry-dependent cancellation effects for spin and charge channels may be a viable way toward an explanation.[78]

C. Properties of the mode in B_{1g} symmetry

Now, the focus will be placed on those properties of the B_{1g} mode appearing below T_c that have not been analyzed previously. In Fig. 3(c), electronic B_{1g} spectra of Bi-2212 are plotted in units of $k_B T_c$. As a general trend, the peaks soften from 9.0 to $4.5 k_B T_c$ for p increasing from 0.15 to 0.23. The variation of the peak energies is not monotonic. For example, the peaks of samples Bi-OPT92, Bi-OPT94, and Bi-OPT96 are at 8.3, 7.3, and $9.0 k_B T_c$, respectively, with T_c and the B_{2g} peaks staying pinned with an accuracy of a few percent. In spite of these differences the normal and superconducting spectra still merge in the same range of 11.5–$13.5\, k_B T_c$ just as in B_{2g} symmetry.

In order to make a connection to previous work, we plot the peak energies $\Omega_{\rm peak}(p)$ for B_{1g} and B_{2g} symmetry in Fig. 4(a). For the range $0.10 \leqslant p \leqslant 0.16$ and for $p \simeq 0.24$, we added data from Ref. 63 to get a more complete picture. Also shown are $2\Delta_0(p) = 9.3\, k_B T_c(p)$ and a linear fit to $\Omega^{B1g}_{\rm peak}(p)$. Here and throughout the paper, $T_c(p)/T_c^{\rm max} = 1 - 82.6(p - 0.16)^2$ as given by Presland *et al.* [48] with $T_c^{\rm max} = 94$ K. Clearly, $\Omega^{B1g}_{\rm peak} = 1294[1 - p/p_0]\,{\rm cm}^{-1}$ with $p_0 = (0.275 \pm 0.020)$ is unrelated to $2\Delta_0(p)$ but extrapolates linearly to the upper critical doping $p_{\rm sc2} \simeq 0.27$ terminating the superconducting dome. In contrast, the peak energies in B_{2g} symmetry scale approximately as $1.3\Delta_0(p)$ where the peak is expected if the lowest order d-wave variation of the gap according to Eq. (1) applies.[42] We note that the effect of impurities on the B_{1g} peak energies would be larger than in B_{2g} symmetry with $\Omega^{B1g}_{\rm peak} \simeq 2\Delta_0 + \Gamma(\Gamma/\Delta_0)$, where Γ is the impurity scattering rate,[67] and just opposite to what is observed.

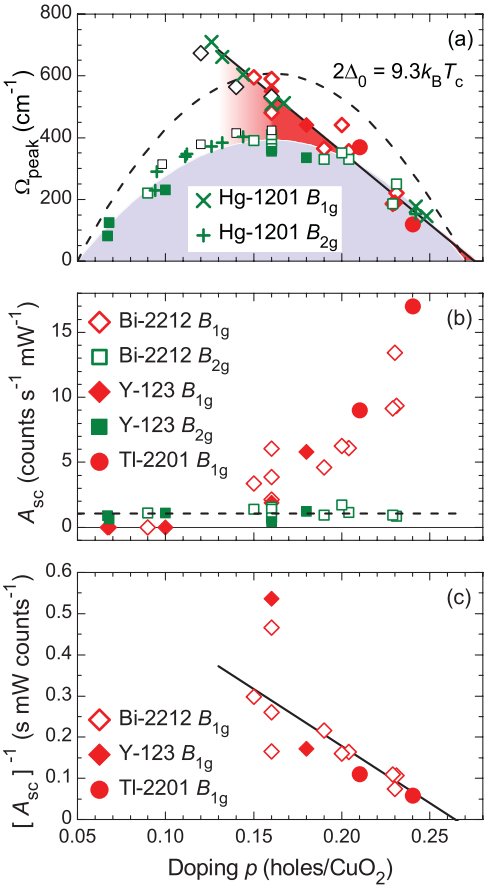

FIG. 4. (Color online) Doping dependence of the superconductivity-induced features in Y-123 (full symbols), Bi-2212 (open symbols), $HgBa_2CuO_{4+\delta}$ (Hg-1201, crosses) and Tl-2201 in B_{1g} symmetry (full circles). The data for Hg-1201 and those of Bi-2212 at $0.10 \leqslant p \leqslant 0.16$ (slightly smaller symbols) are taken from Ref. 63. (a) Peak energies $\Omega_{\rm peak}$. $\Omega^{B2g}_{\rm peak}$ [the crosses are for Hg-1201, other symbols are given in panel (b)] is smaller than $2\Delta_0(p) = 9.3 k_B T_c^{\rm max}[1 - 82.6(p - 0.16)^2]$ with $T_c^{\rm max} = 94$ K (dashes). The same holds true for $\Omega^{B1g}_{\rm peak}$ (diamonds, circles and crosses) at $p > 0.16$. A linear fit to the Bi-2212 data (straight full line) extrapolates to $p_{\rm sc2} \simeq 0.27$. (b) Amplitudes $A_{\rm sc}(p)$ in B_{1g} and B_{2g} symmetries (only our own data). The horizontal line at 1.03 cps/mW is the average of the amplitudes in B_{2g} symmetry. (c) Inverse B_{1g} amplitudes $[A_{\rm sc}(p)]^{-1}$ of Bi-2212, Y-123 and Tl-2201. The linear fit extrapolates to zero at $p \simeq 0.26$ close to $p_{\rm sc2}$.

Now the amplitudes $A_{\rm sc}(p)$ in B_{1g} and B_{2g} symmetry will be analyzed. For doping levels $p \leqslant 0.22$ Blanc and coworkers[38] presented a similar analysis for the B_{1g} spectra and interpreted their results in terms of a gradual loss of coherence close to the $(\pi,0)$ point of the BZ inspired by ARPES results[73] and the discussion of the superfluid density.[6,70] We observe that at doping levels above approximately 0.20 the intensity does not saturate as would be expected from the superfluid density but rather increases at an even higher rate than below 0.20. In Fig. 4(b), we compile results for $A_{\rm sc}(p)$ from the present study on Bi-2212 and Tl-2201 and our earlier results in Y-123[10,14,53] and Bi-2212[10,14,37] with all amplitudes given in

absolute units. (Data from other than our own measurements are not included since intensities from different laboratories cannot be compared.) The differences between Y-123 and Bi-2212 are small, indicating little individual variation for these two double-layer compounds and little influence of resonantly enhanced scattering with excitation in the visible spectral range.[37] For B_{2g} symmetry, $A_{sc}(p)$ is practically doping independent with an average close to 1 count $(\mathrm{s\,mW})^{-1}$. The variations of order $\pm 50\%$ between individual samples (even at similar doping levels) not only reflect impurity effects[67] but also variations of the overall cross section that are not fully understood yet. Similar sample-dependent changes are also observed in B_{1g} symmetry. However, the large basis of results allows us to derive two significant trends: (i) below $p \simeq 0.13$, $A_{sc}(p)$, i.e., any superconductivity-induced spectral change, vanishes in B_{1g} symmetry [cf. Fig. 1(a)] in accordance with earlier studies.[10,14,16,38,62,63] This coincides with the rapid decrease of the coherence peaks in tunneling[27,33,79] and in ARPES at the antinodal Fermi surface crossing.[9,26,31,32] (ii) In Bi-2212 for $p > 0.18$, $A_{sc}(p)$ increases to a degree that has not been appreciated yet. The trend is fully corroborated for samples from one source when studied at various doping levels (see, e.g., Ref. 37). The points from Y-123 and Tl-2201 follow the same trend although issues of oxygen order in the chains lead to strong intensity variations for optimally doped versus fully oxygenated Y-123. If we plot $[A_{sc}(p)]^{-1}$ [see Fig. 4(c)], we find a divergence point at 0.26 ± 0.03 close to $p_{sc2} = 0.27$ where superconductivity disappears (or appears, depending on the point of view).

D. Comparison with other results

Before discussing possible explanations of the increasingly strong B_{1g} mode, it seems instructive to have a closer look at its range of existence and to compare the doping dependence of the Raman results in general with ARPES and tunneling results. We first note that superconductivity-induced features in B_{1g} symmetry exist only in a well-defined range of the doping-energy plane as shown in Fig. 5. For the extremal doping levels ($p \leqslant 0.16$ and $p \sim 0.24$) data from Ref. 63 are included. In addition, the peak energies derived from the superconducting B_{1g} spectra at high pressure are shown.[40] The pressure P in the range up to 22.3 GPa is converted into a doping level p using the linear relation $p = 0.1750 + 0.0028P$ as derived by Goncharov and Struzhkin.[40]

First, there are no B_{1g} modes at energies in excess of approximately $12\,k_B T_c(p)$ where the normal and superconducting spectra are found to merge for those doping levels, where differences can be observed (see Fig. 1). Secondly, none of the peak energies is found outside the range given by the two straight lines obeying $\Omega_L(p) = (1155 - 4279p)$ cm^{-1} and $\Omega_U(p) = (1715 - 6352p)$ cm^{-1} with L (U) denoting the lower (upper) envelope. Although determined by several data points (4–6 each) the lines should be considered more a guide to the eye rather than a fit. Given this qualification, it is nevertheless remarkable that both of them extrapolate to the upper critical doping p_{sc2} in a similar (approximate) fashion as the linear fit to our own data shown in Fig. 4. Up to approximately 10 GPa the peak energies derived from the pressure experiment follow $\Omega_L(p)$ then the doping dependence

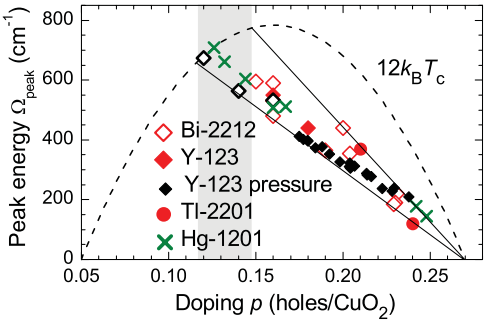

FIG. 5. (Color online) Energy and doping range of the superconductivity-induced B_{1g} features for materials as indicated. The dashed line corresponds to $12\,k_B T_c$, where superconducting and normal-state spectra approximately merge as indicated in Figs. 1, 2, and 3. The black filled diamonds represent results of Raman measurements at high pressure (see Ref. 40) with the doping calculated as described there (see text). All points for Hg-1201 and 3 points for Bi-2212 ($p = 0.12, 0.14, 0.16$, black open diamonds) are taken from Ref. 63. The lower (upper) envelope roughly corresponds to samples with lower (higher) defect concentration and/or internal strain. The shaded area indicates the doping range where the differences between normal-state and superconducting spectra fade away as observed for practically all homogeneous systems.[10,14–16,37,52,62,63]

slightly decreases. As possible reasons, the pressure does not directly correspond to doping or the coefficient may decrease slightly for higher pressure. For instance, a reduction by 20% aligns the peaks with $\Omega_L(p)$. The shaded range in which, depending on the individual sample, the superconductivity-induced features fade away is approximately determined by the intersection points of $\Omega_{L(U)}(p)$ with the energy $12\,k_B T_c(p)$ as expected. It is reemphasized that no changes in the shape and the intensity of the B_{2g} spectra can be observed in this range. Thirdly, $\Omega^{B1g}_{\mathrm{peak}}(p)$ decreases faster than $T_c(p)$ for $0.16 < p \lesssim 0.23$ as demonstrated clearly in the pressure experiment, where the ratio $\Omega^{B1g}_{\mathrm{peak}}(P)/T_c(P)$ decreases from 6.2 to 4.2 in the range 0 to 22.3 GPa corresponding to $p = 0.175$ and 0.24.[40] We consider this observation along with the sample dependence at fixed doping as one indication that the mode in the B_{1g} Raman spectrum is not directly linked to the superconducting gap.

A compilation of tunneling, ARPES, and Raman results is shown in Fig. 6. In the entire overlapping doping range ($0.07 \leqslant p \leqslant 0.19$), $\Omega^{B2g}_{\mathrm{peak}}(p)$ is very similar to the quantity $2\Delta_{sc}$ derived from the nodal part of the single-particle gap as measured by ARPES.[9] $2\Delta_{sc}$ corresponds to $2\Delta_0$ times the fraction of the Fermi surface ℓ_{arc}/ℓ_{FS} on which the observed gap follows the lowest-order d-wave variation as given in Eq. (1). The definitions of Δ_0 and the arc length ℓ_{arc} are shown schematically in the upper left inset of Fig. 6. ℓ_{FS} is the entire length of the Fermi surface. Obviously, Δ_0 is supposed to coincide with the maximal gap according to Eq. (1) while Δ^* is larger than Δ_0. We note that deviations from the lowest-order d-wave variation of the gap were first observed by Mesot *et al.*[80] Yoshida and coworkers[9] interpreted their recent results in terms of two independent gaps Δ_0 and Δ^*, which we followed here. Recently, Chatterjee and collaborators[81] found the gap to obey the lowest-order d-wave form for all doping

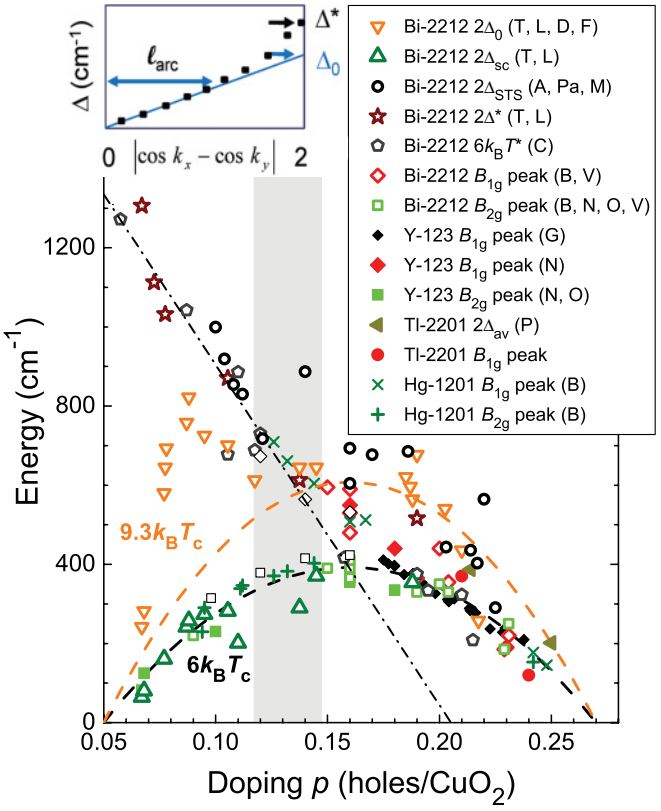

FIG. 6. (Color online) Comparison of tunneling, ARPES, and Raman experiments with the tunneling and ARPES energy scales doubled. All open symbols correspond to Bi-2212. Tunneling results are plotted as open circles. They are compiled from Refs. 8,82, and 83 and labeled as A, Pa, and M, respectively. The stars represent the leading edge midpoints (LEM) measured above T_c at the antinodal Fermi surface crossing and correspond to the pseudogap $2\Delta^*$ (T, Ref. 31 and L, Ref. 32). The pentagons correspond to the crossover temperatures T^* (C, Ref. 29) and are plotted in energy units as $6\,k_B T^*$. The down-pointing triangles represent the gap $2\Delta_0$ derived from ARPES as sketched in the inset according to Ref. 9. The data are compiled from Refs. 31,32,84, and 85. The up-pointing triangles represent $2\Delta_{sc} = 2\Delta_0 \ell_{arc}/\ell_{FS}$, where ℓ_{arc} is defined in the inset and ℓ_{FS} is the full Fermi surface length (T, Ref. 31 and L, Ref. 32). On the overdoped side, ARPES results for Tl-2201 ($p = 0.21$ and 0.25, triangles pointing to the left) are included (P, Ref. 61). Here, the averages of the peak position and the LEM are shown, and the error is on the order of ±20%. The Raman data (approximate peak energies) correspond to those of the previous figures (N, O, V, B, Refs. 10,14,54 and 63). They are similar to within ±20% to those of earlier publications as summarized in Ref. 42 and, more recently, Ref. 63. The high-pressure results are taken from Ref. 40 (G). The dash-dotted line is a fit to $6\,k_B T^*$ and $2\Delta^*$ in the range $p \leqslant 0.16$.

levels indicating that there is still no agreement among the ARPES results.

The tunneling results cover a doping range from 0.100 to 0.225. (All energy scales are doubled as in the case of ARPES.) The results of Alldredge *et al.*[8] and Pasupathy *et al.*[82] are spatially resolved STS data whereas those of Miyakawa and coworkers[83] are not. In the latter case the energies are derived from the peak positions. Since the STS experiments yield location dependent I-V curves there are various approaches to extract a gap as discussed in the respective publications. For the comparison here, we took the maximum of the gap distribution from Ref. 82 and, from Alldredge *et al.*,[8] the gap Δ_1 derived from a d-wave model with impurities. The STS energies are slightly higher but close to those without spatial resolution. Two doping ranges can be distinguished: (i) For $p < 0.13$, the tunneling data follow the line $6\,k_B T^*$. Hence, they are close to those of the antinodal gap Δ^*, which, in the doping range $0.09 \leqslant p \leqslant 0.12$ are slightly above Δ_0 as derived from ARPES. (ii) For $p \geqslant 0.15$, the tunneling results are close to or slightly above $9.3\,k_B T_c(p)$, except for the point at $p = 0.225$ which is approximately at $7\,k_B T_c$.

It appears that more than one half of the ARPES data for Δ_0 and the tunneling results for $p \geqslant 0.15$ follow the line $9.3\,k_B T_c(p)$, as derived from Raman scattering in B_{2g} symmetry, to within the experimental resolution which, for Bi-2212, can be estimated for ARPES close to $p = 0.19$ and for tunneling close to $p = 0.21$ to be of the order of ±10%. Importantly, the ARPES results for Δ_0 follow $9.3\,k_B T_c(p)$ not only close to optimal doping, 0.16 ± 0.04, but also for $p \simeq 0.07$. Major discrepancies are observed in the range $0.08 \leqslant p \leqslant 0.11$ and at 0.22. The ARPES results on Tl-2201,[61] although determined in a different way and with somewhat larger error bars, corroborate those on Bi-2212 and extend the doping to $p = 0.25$. In conclusion, for $0.16 \leqslant p \leqslant 0.21$, the analysis of more recent tunneling, ARPES, and Raman results reveals a significant difference between the maximal gap $\Delta_0(p)$ and the B_{1g} peak energy $\Omega^{B1g}_{peak}(p)$ but consistent values for $\Delta_0(p)$ if the B_{2g} Raman spectra are used. The agreement includes even wider doping ranges if B_{2g} Raman and ARPES data are compared.

Since the glass is apparently more than half full (from the viewpoint of the Raman results), we point out possible reasons for the discrepancies. Most importantly, only in the case of clean isotropic BCS superconductors can the gap be measured directly. In all other cases, the gap parameter or its maximum are derived quantities. Raman scattering measures projections of a coherent superposition of the normal and the anomalous part of the electron's Nambu-Green function, $G_{1,1}$ and $G_{1,2}$, respectively,[42–45] while ARPES (and tunneling spectroscopy) essentially observe $G_{1,1}$ only. Therefore Raman experiments predominantly see the condensate similarly to, for instance, Andreev reflection or optical spectroscopy, and there are good reasons to conclude that the Raman results are closer to the properties of the condensed electrons than single-particle methods. Nevertheless, prominent features in $G_{1,1}$ and $G_{1,2}$ are expected at similar energies at least in the weak coupling approximation. However, in the case of underdoped cuprates with additional instabilities next to superconductivity or, more generally, in strongly interacting anisotropic systems, this assumption is unlikely to hold. For example, there may be an interrelation between the superconducting gap $\Delta_{\mathbf{k}}$ and the pseudogap $\Delta^*_{\mathbf{k}}$ having different dependences on momentum, and the two scales cannot sufficiently be disentangled by only analyzing $G_{1,1}$. This may lead to an overestimation of Δ_0 if Δ^* is larger. Similarly, superconducting fluctuations as reported recently[86] may have an impact on $G_{1,1}$. In the case of the Raman response, $G_{1,2}$ projects mainly the coherent part below T_c and Δ^* loses influence. The solution to this problem is in fact more a theoretical challenge than an experimental one. For

the case where the pseudogap results from a charge-ordering instability, there exist already some studies[87–90] but the way Δ_0 should be extracted from the single-particle spectra needs to be worked out further. This holds also true for other type of excitations that can be at the origin of the pseudogap or appear in the pseudogap range such as magnetic order.[91–93] At high doping, $p \simeq 0.22$, $2\Delta_0$ as derived from ARPES is smaller than $9.3\,k_B T_c(p)$ and appears in the same range of energies as the B_{1g} peaks. The reduction of the energy below $9.3\,k_B T_c(p)$ may start already at 0.21 and is probably related to the presence of the second energy scale observed in the B_{1g} Raman data, which starts close to $2\Delta^*(p)$ near optimal doping and then drops faster than T_c.

$2\Delta^*(p)$, defined as the leading-edge midpoint (LEM) of the energy distribution curve at k_F close to the antinodal point,[9] coincides with $\Omega^{B1g}_{\rm peak}(p)$ in the range $0.12 \leqslant p \leqslant 0.19$ to within the experimental accuracy. Note that $2\Delta^*(p = 0.19)$ is rather high and close to $2\Delta_0$. The crossover temperature $T^*(p)$ below which the pseudogap is observed[29] coincides with $\Omega^{B1g}_{\rm peak}(p)$ in an even wider doping range if it is converted into energies as $6k_B T^*$. Hence, the energy scale $2\Delta^*(p)$ and to some extent also $T^*(p)$, both associated with the pseudogap, have a similar functional dependence on p as $\Omega^{B1g}_{\rm peak}(p)$. However, two important differences should be noticed: (i) The pseudogap becomes unobservable above $p \simeq 0.21$[9,29] whereas the B_{1g} Raman peak gains most of its intensity for $p \geqslant 0.20$. (ii) The doping dependences of $2\Delta^*(p)$ and $6k_B T^*$ change in the range where the Raman peak disappears. The low-doping part of both extrapolates to $p = 0.205 \pm 0.020$ as indicated by a dash-dotted line in Fig. 6 with the functional dependence being represented by $2\Delta^*_<(p) = (1765 - 8606p)$ cm^{-1}. $p \sim 0.2$ is usually identified with p^* and considered a quantum critical point.[5,6,94,95] We note that the onset-temperatures of the hidden magnetic order[91,92] and of the Kerr rotation[93] as well as the charge-ordering tendencies observed in $La_{2-x}Sr_xCuO_4$[68,96] extrapolate to zero at a similar hole concentration $0.18 < p < 0.20$ (for an interpretation see Ref. 95). Both doping levels are significantly below $p_0 \sim 0.27$ derived from $\Omega^{B1g}_{\rm peak}(p)$. Although these general trends have been known for a while the details described here were not yet appreciated. However, we regard them relevant for the clarification of the B_{1g} Raman response.

It is particularly unexpected that the thermal conductivity as a typical low-energy transport probe yields a maximal gap $\Delta_0(p)$ with a functional doping dependence close to that of $\Delta^*(p)$ or $T^*(p)$.[19,21] Here, $\Delta_0(p)$ is determined from the ratio of the perpendicular to the tangential electron velocities, v_F/v_2, at the Fermi surface.[97] Part of the puzzle may be buried in the derivation of v_F from the dispersion $\epsilon_{\mathbf{k}}$ as seen by ARPES. For a long time v_F was believed to be universal and close to 1.5 eV Å (2×10^7 cm s^{-1}).[98] In a recent high-resolution experiment, however, v_F was found to be smaller and to depend on doping.[99] Another part depends on the definition of the superconducting gap and, in particular, its momentum dependence. Finally, if the nodal quasiparticle weight decreases[69] or if part of the carriers do not contribute any further to the heat conduction at low doping, the gap appears to be too large. In any case, the proper interrelation and interpretation of the various experiments and energy scales cannot be finally solved here. From the viewpoint of Raman scattering being sensitive in the spectral range above $\Omega \simeq 15$ cm^{-1} (2 meV), one finds an energy, which scales with T_c and another one with a more linear doping dependence, which we focus on now.

E. Origin of the B_{1g} mode

Given the negligible doping dependence of $f(\mathbf{k})$ and $2\Delta_0/k_B T_c$ as particularly clearly demonstrated by the scaling of the B_{2g} response [see Figs. 3(a) and 3(b)], the variation of $\Omega^{B1g}_{\rm peak}(p)/k_B T_c$ by a factor of two, and the tendency of spectral weight $A^{B1g}_{\rm sc}(p)$ to diverge, it is hard to identify the B_{1g} maximum with Δ_0. What are the alternatives?

An explanation in terms of an exciton-like bound state below $2\Delta_0$ as described first by Bardasis and Schrieffer[100] has been proposed recently.[101,102] It is predicted that a δ-like mode appears below the maximal gap $2\Delta_0$ at $\Omega^{B1g}_{\rm peak} = 2\Delta_0 - E_b$ with the binding energy E_b and the intensity increasing simultaneously with coupling strength α^2_L.[103] In Fig. 7, we plot the dependence of the spectral weight of the in-gap mode on the bound state energy E_b given in units of $k_B T_c$, $E^0_b = E_b/k_B T_c = (2\Delta_0 - \Omega^{B1g}_{\rm peak})/k_B T_c$. E_b is the binding energy of the "Cooperon", an exciton of two electrons bound by particle-particle interactions in a channel L orthogonal to the pairing channel.[45,103–105] This representation demonstrates that the split-off is very small at optimal doping and increases toward higher doping levels. At first glance, the energy and intensity variations predicted on the basis of a spin-fluctuation model are similar to those observed here with a simultaneous increase of both amplitude and split-off below $2\Delta_0$. It is particularly luring that this type of plot partially compensates for the differences between the samples leading to an improved linear scaling, the origin of which has to remain unexplained. However, the doping dependence of the B_{1g} Raman mode is just opposite to what one expects for the spin channel. Similar arguments apply for a bound state induced by charge ordering,[89] since the coupling for both spin and charge

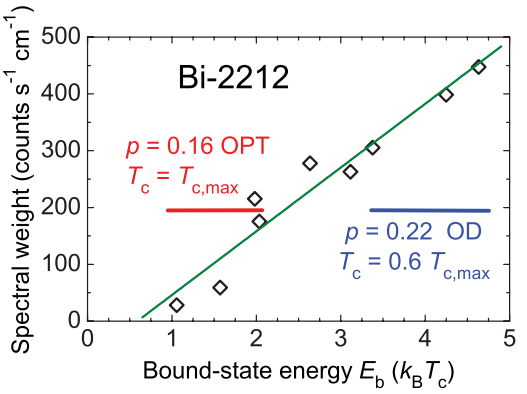

FIG. 7. (Color online) Dependence of the bound state's spectral weight on $E^0_b = (2\Delta_0 - \Omega^{B1g}_{\rm peak})/k_B T_c$ of Bi-2212. The ranges close to optimal doping ($p = 0.16 \pm 0.01$) and at high doping ($p = 0.22 \pm 0.01$) are indicated. Here, the spectral weight is an integral over the in-gap mode alone after subtracting the weak-coupling pair-breaking response from the full response (see also Fig. 8). This can be directly derived from the data shown in Fig. 3(c).

instabilities increases toward low, not high, doping. Similarly, the electron-phonon coupling is expected to increase toward lower carrier concentration due to the reduced screening[106] also in the presence of correlations.[107,108] At present, we are not aware of an interaction with dramatically increasing coupling strength toward high doping.

Alternatively, band structure effects may play a role. A significant increase of the B_{1g} intensity is expected if the van Hove singularity at $(\pi,0)$ approaches and crosses the Fermi level E_F since the Raman cross section is proportional to the density of states at E_F. In LSCO and probably also in Bi-2212, such a crossing is indeed observed.[109] However, Tl-2201 has a holelike Fermi surface at all doping levels as derived from both ARPES[71] and quantum oscillations,[110] and the data on Tl-2201 do not show significant differences to those of Bi-2212. Rather, the doping dependence on the overdoped side turns out to be quite universal[68] and the influence of the van Hove singularity on the superconducting Raman spectra is rather weak.[65] Finally, the quite complicated multisheeted Fermi surface of Y-123 seems to have only little influence on the spectra in the superconducting state. Hence, the synopsis of the results in Bi-2212, Y-123, and Tl-2201 allows us to conclude that band structure effects can be excluded as the origin of the increasing intensity at doping levels above $p = 0.18$. Similarly, the quasiparticle weight saturates above 0.20 toward the mean-field expectation and there is no indication, that the superfluid density increases further for $p > 0.19$ (Refs. 70 and 111).

Since these more traditional possibilities fail to provide a qualitatively correct description of the experiments, we explore a scenario that rests on the unconventional evolution with doping of the B_{1g} intensity. If individual variations between the samples are neglected, $A_{\rm sc}^{B1g}(p)$ diverges approximately as

$$A_{\rm sc}^{B1g}(p) \propto (1 - p/p_{\rm sc2})^{-1}. \qquad (3)$$

Although the quasiparticles at the antinode become substantially sharper upon overdoping, such as observed by ARPES particularly in the case of Tl-2201 at $p = 0.25$,[71] the evolution of the B_{1g} Raman response can hardly be explained in this way. If this were the case, the B_{1g} maximum would just become narrower while conserving the integrated area.

The observed intensity increase along with the reduction of $\Omega_{\rm peak}^{B1g}(p)$ [see Fig. 4(a)] is instead more compatible with the behavior of a Goldstone mode appearing when a continuous symmetry is broken.[112,113] Such a scenario was actually suggested to be a possible explanation of the π resonance at low doping in the SO(5) scenario.[114] Qualitatively, the B_{1g} Raman mode exhibits an analogous doping dependence toward $p_{\rm sc2}$. In fact, we not only find $A_{\rm sc}^{B1g}(p)$ to diverge at $p = 0.26 \pm 0.03$ but also $\Omega_{\rm peak}^{B1g}(p)$ to extrapolate linearly to zero at $p = 0.27 \pm 0.02$ as expected for a symmetry-breaking mode.

In this scenario, the B_{1g} spectrum is a superposition of the weak-coupling pair-breaking feature (having, however, a substantially increased $2\Delta_0/k_BT_c$ ratio) and an additional mode with B_{1g} symmetry originating from a broken continuous symmetry. This would, in a natural way, explain the strong energy dependence of the transient amplitude of the B_{1g} pair-breaking feature observed in the time domain,[115]

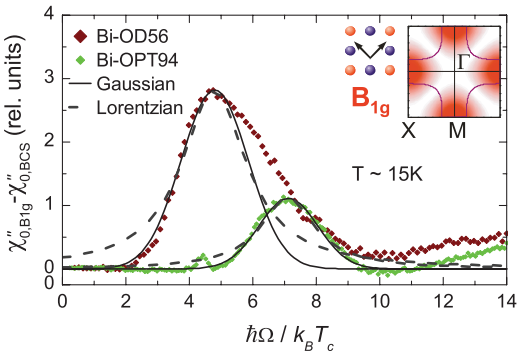

FIG. 8. (Color online) Analysis of the spectral shape of the extra contribution to the superconducting B_{1g} response in Bi-2212. The spectra are derived from those in Fig. 3(c) by subtracting the weak-coupling result [dashed line in Fig. 3(c)]. The solid line represents a Gaussian, the dashed one a Lorentzian. Except for the highest doping level of 0.23, all spectra are similarly well fit by Gaussians as the one at optimal doping.

which was in fact interpreted in terms of a two-component response. The superposition can be explored quantitatively for Bi-2212 since the weak-coupling BCS prediction can directly be subtracted from the spectra as shown in Fig. 8. The resulting peak has a purely Gaussian lineshape for $0.16 \leqslant p \leqslant 0.21$. For higher doping levels, deviations on the high-energy side are observed resulting either from inhomogeneities of the doping level, which are very likely for $p > 0.21$ or from an interaction of the mode with the in-gap states. In none of the cases, a Lorentzian line shape is compatible with the data. Usually, a Gaussian is indicative of inhomogeneous broadening rather than a finite lifetime. The additional response is then a superposition of lines at statistically distributed energies with relatively narrow if not resolution-limited width. This would trace back the strong sample dependences to strain fields from disorder or insufficient relaxation of the structure.[46] In fact, the pressure experiments directly show the susceptibility of $\Omega_{\rm peak}^{B1g}/k_BT_c$ to stress.[40]

The microscopic origin remains elusive. Light scattering from a spin-density modulation with $\mathbf{q} = (\pi,\pi)$ or from the celebrated π resonance[116–118] would not appear in B_{1g} but, rather, in A_{1g} symmetry[119,120] and is, therefore, unlikely to be the origin of the B_{1g} mode. Similar symmetry arguments apply for the weakly dispersive magnetic modes that were discovered recently below T^* (Ref. 121) and interpreted in terms of loop currents.[122,123] Scattering on one of these excitations would actually appear in A_{2g} symmetry because of their chiral character.[122] Combined neutron and Raman scattering experiments on $HgBa_2CuO_4$ could help clarifying this issue. A Pomeranchuk instability of the Fermi surface[124,125] or spin and/or charge ordering fluctuations with ordering vector $\mathbf{Q} = (0.2\pi,0)$[126,127] would have the proper symmetry. However, only the coupling of two fluctuations would guarantee to satisfy the $q = 0$ selection rule of light scattering in the normal and in the superconducting state. Recently, the direct coupling between the charge density wave and the superconducting gap has been studied by ARPES.[90] This could be a possible solution for doping levels below $p \sim 0.2$ as pointed out already by Benfatto and coworkers[88] and Zeyher and Greco[89]

whereas higher doping levels with very short-range order have not been explored yet. Finally, the mode could be a critical mode of a nematic phase being established at the onset of superconductivity at $p_{sc2} \simeq 0.27$.[128,129] For symmetry reasons, charge-ordering fluctuations or electronic nematic order are the most probable candidates. While indications of charge order were observed in $La_{2-x}Sr_xCuO_4$ (Ref. 126), their relevance for the high-T_c compounds is not clear. In all cases, the mode is closely related to superconductivity without, however, being linked to the energy gap.

The experiments suggest a smooth transition between the energies $\Omega_{\rm peak}^{B1g}$ and $2\Delta^*$ close to optimal doping. Whether or not the similarity of the energy scales is just accidental or indicative of a relationship between the pseudogap and the putative symmetry breaking occurring at p_{sc2} is among the tantalizing open questions highlighted by this study. Yet, the present theoretical understanding is too limited to arrive at an answer.

V. CONCLUSIONS

We have measured and analyzed the superconducting Raman response in Bi-2212, Y-123, and Tl-2201 single crystals. The present results are compared to existing data from our own work and from the literature. In Bi-2212, close to optimal doping the material dependence of the B_{1g} spectra was scrutinized revealing a significant variation with the samples' origin and history. Tl-2201 and Y-123 were used to get insight into more extreme doping levels on the over- and under-doped sides, respectively. Superconductivity-induced features could be observed in B_{1g} and B_{2g} symmetries in the doping ranges $0.15 \leqslant p \leqslant 0.24$ and $0.07 \leqslant p \leqslant 0.23$, respectively.

The scaling with the experimentally determined transition temperature T_c of the entire B_{2g} pair-breaking spectra, which by and large measure the condensate, is one of the central results of this publication and pins down the superconducting gap's momentum dependence to be close to the lowest order $d_{x^2-y^2}$ form in the doping range $0.07 \leqslant p \leqslant 0.23$. The gap ratio $2\Delta_0/k_BT_c \simeq 9.3$ is much higher than the BCS weak-coupling result and is found to not depend on doping. The scaling of not only the peak frequencies but also the complete B_{2g} spectra and the weak doping dependence of the overall intensity do not support a compensation effect between the gap magnitude and the loss of coherence on the antinodal parts of the Fermi surface as proposed recently.[63] Rather, the Raman results suggest that the near-nodal electronic states of the condensate exhibit BCS-type properties and seem to be protected by symmetry. Yet, there is no convincing explanation why the light scattering response does not reflect the reduction of the nodal quasiparticle weight Z_N observed by ARPES.[69] Similarly, there is no conclusive answer as to why the heat transport as a typical low-energy probe reflects the large gap following $(1 - p/p_{sc2})$[19,20] and why the gap derived from the single-particle spectra[9,99] has a quite complicated doping dependence with a maximum close to $p = 0.09$. More generally, there remain considerable discrepancies between different methods probing $\Delta_{\mathbf{k}}$, which apparently go beyond the conventional understanding, even in the limit of strong coupling, and need further attention.

The variations of energy and amplitude of the superconductivity-induced B_{1g} spectra cannot originate from a doping dependence of the gap beyond the approximate scaling with T_c of Δ_0, since there should also be an influence on the B_{2g} spectra. For $p > 0.16$, we are apparently dealing with a mode of well defined B_{1g} symmetry (typical for a collective mode) rather than a projection of the gap as in B_{2g} symmetry. We speculate that the mode indicates a continuous symmetry to be broken at the onset point of superconductivity at $p_{sc2} \simeq 0.27$. Possible candidates are the fluctuating spin and charge textures with finite q (Refs. 127 and 130), a Pomeranchuk instability of the Fermi surface,[124] or nematic charge order at $q = 0$ (Ref. 128). In all cases the damping is reduced for energies smaller than $2\Delta_0$. Possible signatures of antiferromagnetism or orbital currents are expected in A_{1g} and A_{2g} symmetry, respectively, and are therefore unlikely to be an explanation of the B_{1g} Raman response. If the coincidence of the energies $\Omega_{\rm peak}^{B1g}$ and $2\Delta^*$ occurring close to optimal doping is not just accidental, the results indicate a relationship between the broken symmetry and the pseudogap. It is an intriguing possibility that the B_{1g} mode is related to the fluctuation spectrum at the origin of superconductivity.

ACKNOWLEDGMENTS

We thank A. Auerbach, T. P. Devereaux, S. A. Kivelson, Yuan Li, I. M. Vishik, and Guichuan Yu for valuable discussions and comments. R. H. acknowledges the hospitality of the Geballe Laboratory of Advanced Materials at Stanford University where part of the paper was completed. We acknowledge support by the DFG under Grant Nos. HA 2071/3 and ER 342/1 via Research Unit FOR 538 and via the Collaborative Research Centre TRR 80. The crystal growth work at Stanford and Vancouver was supported by DOE under Contract No. DE-AC03-76SF00515 and by NSERC Canada, respectively.

*Present address: Max Planck Institute for Solid State Research, 70569 Stuttgart, Germany.
†Present address: Mettler-Toledo (Schweiz) GmbH, 8606 Greifensee, Switzerland.
‡Present address: MBDA, 86529 Schrobenhausen, Germany.
§Present address: GP Inspect GmbH, 82152 Planegg/Martinsried, Germany.
‖The crystal growth work was performed in M.G.'s previous laboratory at Stanford University, Stanford, CA 94305, USA.

[1] C. C. Tsuei and J. R. Kirtley, Rev. Mod. Phys. **72**, 969 (2000).
[2] D. J. Scalapino, E. Loh, and J. E. Hirsch, Phys. Rev. B **34**, 8190 (1986).
[3] P. A. Lee, N. Nagaosa, and X.-G. Wen, Rev. Mod. Phys. **78**, 17 (2006).

[4]P. W. Anderson, Science **316**, 1705 (2007).
[5]T. Timusk and B. Statt, Rep. Prog. Phys. **62**, 61 (1999).
[6]J. L. Tallon and J. W. Loram, Physica C **349**, 53 (2001).
[7]M. R. Norman, D. Pines, and C. Kallin, Adv. Phys. **54**, 715 (2005).
[8]J. W. Alldredge *et al.*, Nat. Phys. **4**, 319 (2008).
[9]T. Yoshida *et al.*, Phys. Rev. Lett. **103**, 037004 (2009).
[10]R. Nemetschek, M. Opel, C. Hoffmann, P. F. Müller, R. Hackl, H. Berger, L. Forrò, A. Erb, and E. Walker, Phys. Rev. Lett. **78**, 4837 (1997).
[11]L. V. Gasparov, P. Lemmens, N. N. Kolesnikov, and G. Güntherodt, Phys. Rev. B **58**, 11753 (1998).
[12]C. Panagopoulos and T. Xiang, Phys. Rev. Lett. **81**, 2336 (1998).
[13]G. Deutscher, Nature (London) **397**, 410 (1999).
[14]M. Opel *et al.*, Phys. Rev. B **61**, 9752 (2000).
[15]S. Sugai and T. Hosokawa, Phys. Rev. Lett. **85**, 1112 (2000).
[16]M. Le Tacon *et al.*, Nature Physics **2**, 537 (2006).
[17]M. Chiao, R. W. Hill, C. Lupien, L. Taillefer, P. Lambert, R. Gagnon, and P. Fournier, Phys. Rev. B **62**, 3554 (2000).
[18]J. Takeya, Y. Ando, S. Komiya, and X. F. Sun, Phys. Rev. Lett. **88**, 077001 (2002).
[19]M. Sutherland *et al.*, Phys. Rev. B **67**, 174520 (2003).
[20]D. G. Hawthorn *et al.*, Phys. Rev. B **75**, 104518 (2007).
[21]L. Taillefer, Annu. Rev. Cond. Mat. Phys. **1**, 51 (2010).
[22]C. C. Homes, T. Timusk, R. Liang, D. A. Bonn, and W. N. Hardy, Phys. Rev. Lett. **71**, 1645 (1993).
[23]A. G. Loeser *et al.*, Science **273**, 325 (1996).
[24]H. Ding, M. R. Norman, J. C. Campuzano, M. Randeria, A. F. Bellman, T. Yokoya, T. Takahashi, T. Mochiku, and K. Kadowaki, Phys. Rev. B **54**, R9678 (1996).
[25]S. Hüfner, M. A. Hossain, A. Damascelli, and G. A. Sawatzky, Rep. Prog. Phys. **71**, 062501 (2008).
[26]A. Damascelli, Z. Hussain, and Z.-X. Shen, Rev. Mod. Phys. **75**, 473 (2003).
[27]K. K. Gomes *et al.*, Nature (London) **447**, 569 (2007).
[28]C. Renner, B. Revaz, J. Y. Genoud, K. Kadowaki, and Ø. Fischer, Phys. Rev. Lett. **80**, 149 (1998).
[29]J. C. Campuzano *et al.*, Phys. Rev. Lett. **83**, 3709 (1999).
[30]C. Kendziora and A. Rosenberg, Phys. Rev. B **52**, 9867 (1995).
[31]K. Tanaka *et al.*, Science **314**, 1910 (2006).
[32]W. S. Lee *et al.*, Nature (London) **450**, 81 (2007).
[33]K. McElroy, D. H. Lee, J. E. Hoffman, K. M. Lang, J. Lee, E. W. Hudson, H. Eisaki, S. Uchida, and J. C. Davis, Phys. Rev. Lett. **94**, 197005 (2005).
[34]O. K. Andersen, A. I. Liechtenstein, O. Jepsen, and F. Paulsen, J. Phys. Chem. Solids **56**, 1573 (1995).
[35]C. Bernhard, R. Henn, A. Wittlin, M. Klaser, T. Wolf, G. Muller-Vogt, C. T. Lin, and M. Cardona, Phys. Rev. Lett. **80**, 1762 (1998).
[36]J. G. Naeini, X. K. Chen, J. C. Irwin, M. Okuya, T. Kimura, and K. Kishio, Phys. Rev. B **59**, 9642 (1999).
[37]F. Venturini *et al.*, J. Phys. Chem. Solids **63**, 2345 (2002).
[38]S. Blanc, Y. Gallais, A. Sacuto, M. Cazayous, M. A. Mèasson, G. D. Gu, J. S. Wen, and Z. J. Xu, Phys. Rev. B **80**, 140502 (2009).
[39]Y. Kohsaka *et al.*, Nature (London) **454**, 1072 (2008).
[40]A. Goncharov and V. Struzhkin, J. Raman Spectrosc. **34**, 532 (2003).
[41]S. Sadewasser, J. S. Schilling, A. P. Paulikas, and B. W. Veal, Phys. Rev. B **61**, 741 (2000).
[42]T. Devereaux and R. Hackl, Rev. Mod. Phys. **79**, 175 (2007).
[43]A. A. Abrikosov and L. A. Fal'kovskii, Zh. Eksp. Teor. Fiz. **40**, 262 (1961); Sov. Phys. JETP **13**, 179 (1961).
[44]A. Abrikosov and V. Genkin, Zh. Eksp. Teor. Fiz. **65**, 842 (1973) [Sov. Phys. JETP **38**, 417 (1974)].
[45]M. V. Klein and S. B. Dierker, Phys. Rev. B **29**, 4976 (1984).
[46]H. Eisaki, N. Kaneko, D. L. Feng, A. Damascelli, P. K. Mang, K. M. Shen, Z.-X. Shen, and M. Greven, Phys. Rev. B **69**, 064512 (2004).
[47]D. Peets *et al.*, J. Cryst. Growth **312**, 344 (2010).
[48]M. R. Presland *et al.*, Physica C **176**, 95 (1991).
[49]R. Liang, D. A. Bonn, and W. N. Hardy, Phys. Rev. B **73**, 180505 (2006).
[50]A. Erb, E. Walker, and R. Flükiger, Physica C **258**, 9 (1996).
[51]R. Liang, D. A. Bonn, and W. N. Hardy, Physica C **304**, 105 (1998).
[52]X. K. Chen, J. G. Naeini, K. C. Hewitt, J. C. Irwin, R. Liang, and W. N. Hardy, Phys. Rev. B **56**, R513 (1997).
[53]R. Nemetschek *et al.*, Eur. Phys. J. B **5**, 495 (1998).
[54]F. Venturini, M. Opel, T. P. Devereaux, J. K. Freericks, I. Tüttő, B. Revaz, E. Walker, H. Berger, L. Forró, and R. Hackl, Phys. Rev. Lett. **89**, 107003 (2002).
[55]M. Schneider, R.-S. Unger, R. Mitdank, R. Müller, A. Krapf, S. Rogaschewski, H. Dwelk, C. Janowitz, and R. Manzke, Phys. Rev. B **72**, 014504 (2005).
[56]D. C. Peets *et al.*, Phys. Rev. Lett. **103**, 087402 (2009).
[57]M. Kang, G. Blumberg, M. V. Klein, and N. N. Kolesnikov, Phys. Rev. Lett. **77**, 4434 (1996).
[58]C. Kendziora, R. J. Kelley, and M. Onellion, Phys. Rev. Lett. **77**, 727 (1996).
[59]N. N. Kolesnikov *et al.*, Physica C **195**, 219 (1992).
[60]J. L. Wagner *et al.*, Physica C **277**, 170 (1997).
[61]D. C. Peets *et al.*, New J. Phys. **9**, 28 (2007).
[62]R. Hackl *et al.*, in *Advanced Solid State Physics*, edited by B. Kramer, Vol. 45 (Springer, Berlin-Heidelberg, 2005), pp. 227–238.
[63]S. Blanc, Y. Gallais, M. Cazayous, M. A. Méasson, A. Sacuto, A. Georges, J. S. Wen, Z. J. Xu, G. D. Gu, and D. Colson, Phys. Rev. B **82**, 144516 (2010).
[64]T. P. Devereaux, D. Einzel, B. Stadlober, R. Hackl, D. H. Leach, and J. J. Neumeier, Phys. Rev. Lett. **72**, 396 (1994).
[65]W. Prestel *et al.*, Eur. Phys. J. Special Topics **188**, 163 (2010).
[66]D. S. Inosov *et al.*, Phys. Rev. B **77**, 212504 (2008).
[67]T. P. Devereaux, Phys. Rev. Lett. **74**, 4313 (1995).
[68]B. Muschler *et al.*, Eur. Phys. J. Special Topics **188**, 131 (2010).
[69]D. Fournier *et al.*, Nat. Phys. **6**, 905 (2010).
[70]D. L. Feng *et al.*, Science **289**, 277 (2000).
[71]M. Platé *et al.*, Phys. Rev. Lett. **95**, 077001 (2005).
[72]M. R. Norman *et al.*, Nature (London) **392**, 157 (1998).
[73]T. Yoshida *et al.*, Phys. Rev. Lett. **91**, 027001 (2003).
[74]J. Chang *et al.*, Phys. Rev. B **78**, 205103 (2008).
[75]L. Tassini, W. Prestel, A. Erb, M. Lambacher, and R. Hackl, Phys. Rev. B **78**, 020511 (2008).
[76]G. Blumberg and M. V. Klein, J. Low Temp. Phys. **117**, 1001 (1999).
[77]E. Gull, M. Ferrero, O. Parcollet, A. Georges, and A. J. Millis, Phys. Rev. B **82**, 155101 (2010).

[78]C. Di Castro, B. Muschler, W. Prestel, R. Hackl, M. Lambacher, A. Erb, S. Komiya, Y. Ando, and M. Grilli, Phys. Rev. B **84**, 054508 (2011).
[79]A. Pushp *et al*., Science **324**, 1689 (2009).
[80]J. Mesot *et al*., Phys. Rev. Lett. **83**, 840 (1999).
[81]U. Chatterjee *et al*., Nat. Phys. **6**, 99 (2010).
[82]A. N. Pasupathy *et al*., Science **320**, 196 (2008).
[83]N. Miyakawa, J. F. Zasadzinski, L. Ozyuzer, P. Guptasarma, D. G. Hinks, C. Kendziora, and K. E. Gray, Phys. Rev. Lett. **83**, 1018 (1999).
[84]H. Ding, J. R. Engelbrecht, Z. Wang, J. C. Campuzano, S.-C. Wang, H.-B. Yang, R. Rogan, T. Takahashi, K. Kadowaki, and D. G. Hinks, Phys. Rev. Lett. **87**, 227001 (2001).
[85]D. L. Feng *et al*., Phys. Rev. Lett. **86**, 5550 (2001).
[86]A. Dubroka *et al*., Phys. Rev. Lett. **106**, 047006 (2011).
[87]E. Cappelluti and R. Zeyher, Phys. Rev. B **59**, 6475 (1999).
[88]L. Benfatto, S. Caprara, and C. Di Castro, Eur. Phys. J. B **17**, 95 (2000).
[89]R. Zeyher and A. Greco, Phys. Rev. Lett. **89**, 177004 (2002).
[90]R.-H. He *et al*., Science **331**, 1579 (2011).
[91]B. Fauqué, Y. Sidis, V. Hinkov, S. Pailhès, C. T. Lin, X. Chaud, and P. Bourges, Phys. Rev. Lett. **96**, 197001 (2006).
[92]Y. Li *et al*., Nature (London) **455**, 372 (2008).
[93]J. Xia *et al*., Phys. Rev. Lett. **100**, 127002 (2008).
[94]C. M. Varma, P. B. Littlewood, S. Schmitt-Rink, E. Abrahams, and A. E. Ruckenstein, Phys. Rev. Lett. **63**, 1996 (1989).
[95]S. Andergassen, S. Caprara, C. Di Castro, and M. Grilli, Phys. Rev. Lett. **87**, 056401 (2001).
[96]L. Tassini, F. Venturini, Q.-M. Zhang, R. Hackl, N. Kikugawa, and T. Fujita, Phys. Rev. Lett. **95**, 117002 (2005).
[97]A. C. Durst and P. A. Lee, Phys. Rev. B **62**, 1270 (2000).
[98]X. J. Zhou *et al*., Nature (London) **423**, 398 (2003).
[99]I. M. Vishik *et al*., Phys. Rev. Lett. **104**, 207002 (2010).
[100]A. Bardasis and J. R. Schrieffer, Phys. Rev. **121**, 1050 (1961).
[101]A. V. Chubukov, T. P. Devereaux, and M. V. Klein, Phys. Rev. B **73**, 094512 (2006).
[102]A. V. Chubukov and M. R. Norman, Phys. Rev. B **77**, 214529 (2008).
[103]H. Monien and A. Zawadowski, Phys. Rev. B **41**, 8798 (1990).
[104]A. Zawadowski, J. Ruvalds, and J. Solana, Phys. Rev. A **5**, 399 (1972).
[105]T. P. Devereaux and D. Einzel, Phys. Rev. B **51**, 16336 (1995).
[106]D. Johnston, Adv. Phys. **59**, 803 (2010).
[107]M. Grilli and C. Castellani, Phys. Rev. B **50**, 16880 (1994).
[108]Z. B. Huang, W. Hanke, E. Arrigoni, and D. J. Scalapino, Phys. Rev. B **68**, 220507 (2003).
[109]T. Yoshida *et al*., Phys. Rev. B **74**, 224510 (2006).
[110]N. Hussey, Eur. Phys. J. B **31**, 495 (2003).
[111]C. Bernhard, J. L. Tallon, Th. Blasius, A. Golnik, and Ch. Niedermayer, Phys. Rev. Lett. **86**, 1614 (2001).
[112]J. Goldstone, A. Salam, and S. Weinberg, Phys. Rev. **127**, 965 (1962).
[113]N. Nagaosa, *Quantum Field Theory in Condensed Matter Physics* (Springer, Berlin-Heidelberg, 1999).
[114]E. Demler, W. Hanke, and S.-C. Zhang, Rev. Mod. Phys. **76**, 909 (2004).
[115]R. P. Saichu *et al*., Phys. Rev. Lett. **102**, 177004 (2009).
[116]H. A. Mook, M. Yethiraj, G. Aeppli, T. E. Mason, and T. Armstrong, Phys. Rev. Lett. **70**, 3490 (1993).
[117]V. Hinkov *et al*., Nature (London) **430**, 650 (2004).
[118]G. Yu, Y. Li, E. M. Motoyama, and M. Greven, Nat. Phys. **5**, 873 (2009).
[119]F. Venturini, U. Michelucci, T. P. Devereaux, and A. P. Kampf, Phys. Rev. B **62**, 15204 (2000).
[120]Y. Gallais, A. Sacuto, P. Bourges, Y. Sidis, A. Forget, and D. Colson, Phys. Rev. Lett. **88**, 177401 (2002).
[121]Y. Li *et al*., Nature (London) **468**, 283 (2010) and manuscript in preparation.
[122]V. Aji and C. M. Varma, Phys. Rev. Lett. **99**, 067003 (2007).
[123]Y. He and C. M. Varma, Phys. Rev. Lett. **106**, 147001 (2011).
[124]W. Metzner, D. Rohe, and S. Andergassen, Phys. Rev. Lett. **91**, 066402 (2003).
[125]H. Yamase and R. Zeyher, Phys. Rev. B **83**, 115116 (2011).
[126]S. Wakimoto, H. Zhang, K. Yamada, I. Swainson, Hyunkyung Kim, and R. J. Birgeneau, Phys. Rev. Lett. **92**, 217004 (2004).
[127]S. Caprara, C. Di Castro, M. Grilli, and D. Suppa, Phys. Rev. Lett. **95**, 117004 (2005).
[128]S. A. Kivelson *et al*., Rev. Mod. Phys. **75**, 1201 (2003).
[129]W.-C. Lee, S.-C. Zhang, and C. Wu, Phys. Rev. Lett. **102**, 217002 (2009).
[130]J. Tranquada, in *Handbook of High-Temperature Superconductivity Theory and Experiment*, edited by J. Schrieffer and J. Brooks (Springer, Berlin-Heidelberg, 2007).